



## LETTER

# The germline genetics of mild-to-moderate penetrance: An intriguing role of *PRAME* in multiple carcinogenesis

Germline genetics of high penetrance such as *BRCA* genes, mutations might be sufficient for carcinogenesis, but this only explains fewer than 10% of cancers. We assume that most cancers are the result of germline mutations of low to moderate penetrance, combined with acquired mutations due to external carcinogenic stressors. With their accumulation over time, aging is associated with an increased risk of multiple cancer development in a given individual. For decades, germline genetics have been based on familial linkage studies enabling most high-penetrance genes to be identified. More recently, population-wide studies have led to the identification of considerable numbers of polymorphisms associated with cancer risk. However, most of them are of unknown functional value, thus limiting their translational application.

Recently, we achieved proof of concept in an individual approach: in a young woman with a history of breast cancer, myeloproliferative disorder, and rheumatoid arthritis not arising from a known genetic syndrome, we identified a germline *MET* mutation of unknown functional significance. The transgenic mouse model that we obtained for this *MET* mutation reproduced the patient's diseases and for the first time established a genetic link between auto-immune diseases and malignancies.<sup>1</sup> This success led us to apply the same individual approach to a 70-year-old woman with a history of multiple cancers over 30 years.

In a single-center database of 447 cancer patients, 70 patients (15.6%) had at least two different cancers, most of them with no predisposing genetic syndrome (Table S1). In particular, Ms. X had an intriguing personal history of 6 different cancers diagnosed between the ages of 39 and 70 years. Despite a familial cancer history over three generations, including breast, ovarian, colon, and thyroid cancers (Fig. 1A), no syndrome predisposing to cancer was identified, including *BRCA1/2*, *Li-Fraumeni*, *Cowden*, or *HNPCC* syndromes. A total

of 6 tumor samples were available, including three formalin-fixed samples for the breast, thyroid, and kidney tumors, and three frozen samples for the three breast cancers. In all cases, tumor cells were selected by laser-microdissection for further DNA extraction. With the patient's consent, we also obtained her germline DNA from peripheral blood mononuclear cells. Two complementary whole-genome analysis methods were used: i) next-generation sequencing (NGS) for the three frozen samples and germline DNA, and ii) OncoScan™ gene hybridization for the three formalin-fixed samples (supplementary methods; Fig. S1).

Using OncoScan™ technology, we did not find any hot-spot mutation among the 9 genes analyzed (*BRAF*, *KRAS*, *EGFR*, *IDH1*, *IDH2*, *PTEN*, *PIK3CA*, *NRAS*, and *TP53*). For copy number alterations, we identified two loss-of-heterozygosity regions (LOH) common to the three tumor samples, and thus considered them to be germline abnormalities, in cytobands 4p21.3 – q22.1 and 22q11.1 – q11.23 (Fig. 1B; Fig. S2 and Table S2). Whereas the second LOH includes the region implicated in 22q11.2 deletion syndrome, our patient did not have any typical symptoms of 22q11.2 deletion/Di-Georges syndrome. This region comprises 416 genes, including several genes with carcinogenic potential, such as *BID*, *BCR*, or *PRAME*.

Using NGS, we first analyzed the mutational profiles of the 3 breast tumor samples. We found a low tumor mutational burden of 2.13 mutations per Mega base. For each of the three samples, we identified a different pathogenic mutation of *PIK3CA* (Fig. S3 and Table S3–7). We then analyzed the constitutional DNA and found five successive regions of LOH on chromosome 22 (calculated copy number < 2) with a total length of more than 8 Mb (15 528 649–21 213 133), and corresponding more or less to the LOH identified using OncoScan™ (16 054 713–24 341 388). Otherwise, we did not find any mutation in genes involved in known syndromes predisposing to cancer (Table S8). For variant analysis (Table S9), we used a frequency threshold of 0.1% or less in the 1000 Genomes,

Peer review under responsibility of Chongqing Medical University.

<https://doi.org/10.1016/j.gendis.2023.04.034>

2352-3042/© 2023 The Authors. Publishing services by Elsevier B.V. on behalf of KeAi Communications Co., Ltd. This is an open access article under the CC BY-NC-ND license (<http://creativecommons.org/licenses/by-nc-nd/4.0/>).

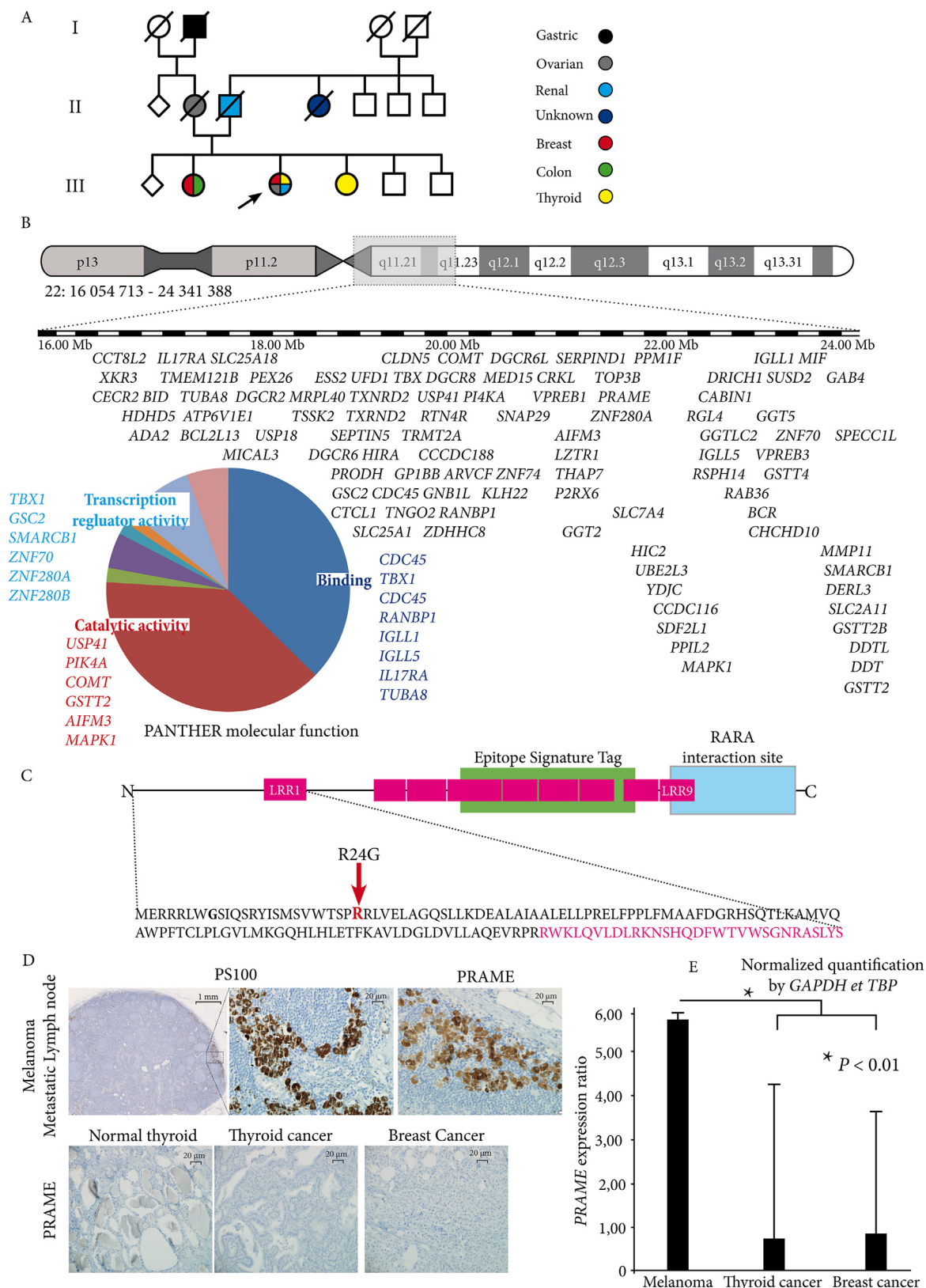


**Figure 1** PRAME at the cornerstone of a case with multiple carcinogenesis. **(A)** Genealogic tree. **(B)** Region of LOH on chromosome 22 in breast, thyroid, and oncocytoma tumor samples using OncoScan™, with corresponding genes and their functional classification. **(C)** Structure of the PRAME protein. The arrow shows the protein modification linked to the c.70 C>G p.Arg24Gly PRAME mutation. **(D)** Immunostaining for PRAME and PS100 in the breast and thyroid cancers of our patient. A melanoma lymph node metastasis is used as a positive control. Bar scale = 20 μm. **(E)** RTqPCR on laser-microdissected cells shows almost no mRNA expression of PRAME in the breast and thyroid cancer cells of our patient, compared with melanoma cells (error bars with a standard deviation of 5%). \* $P < 0.01$ .

GenomeAD, and Kaviar databases to eliminate polymorphisms. We identified two potential mutations in genes located in the 22q11.1 – q11.23 region: i) NM\_001122731.2: c.1450-22T>G of *MICAL3* (Microtubule Associated Monooxygenase, Calponin And LIM domain Containing 3), ii) NM\_006115.4: c.70C>G of *PRAME* (PReferentially expressed Antigen in MElanoma). Since the *MICAL3* variant was intronic, we chose to focus on the *PRAME* gene mutation. NGS analysis included 11 transcripts of *PRAME*: NM\_006115.4, NM\_001291716.1, NM\_206953.2, NM\_206954.2, NM\_001291717.1, NM\_206955.2, NM\_206956.2, NM\_001291719.1, NM\_001318126.1, NM\_001291715.1, NM\_001318127.1.

Overall, considering the low tumor mutational burden, the 22q11.1 – q11.23 LOH region which comprises the *PRAME* gene, and the single *PRAME* germline variant, we hypothesized that this variant was pathogenic and that this equivalence of *PRAME* homozygous deletion and loss of function at protein level was implicated in the multiple carcinogenesis of our patient. The association between *PRAME* mRNA expression and its carcinogenic role is controversial. *PRAME* overexpression seems to be associated with a metastatic phenotype and advanced stages of cancers.<sup>2</sup> This c.70C>G p.Arg24Gly *PRAME* mutation is of unknown functional significance. It is located on the N-terminal side, outside the epitope signature tag (Fig. 1C), and leads to the replacement of the arginine in position 24 with a glycine. The first is an amphipathic polar amino acid frequent in active or binding sites, while the second is a smaller nonpolar amino acid capable of binding phosphates in ATP. In addition, glycine to arginine changes, especially in transmembrane regions of membrane-bound proteins, can modify protein folding and can be associated with diseases.<sup>3</sup>

We then assessed the protein expression level of *PRAME* in two cancer samples from our patient using immunohistochemistry and an anti-*PRAME* antibody that recognizes an epitope including this mutated form of *PRAME* protein (supplementary methods). Compared with a melanoma lymph node metastasis used as a positive control, we did not find any *PRAME* protein expression in the thyroid and breast cancers of our patient (Fig. 1D). Using digital droplet PCR on laser-microdissected tumor cells, we also found very low *PRAME* mRNA expression in the breast and thyroid cancer cells compared with melanoma cells (Fig. 1E). Altogether, these results showed that this c.70C>G p.Arg24Gly variant could be a loss-of-function mutation leading to an undetectable level of mRNA and protein expression.

To address the early carcinogenic potential of this mutation, we developed two knockout (KO) clones of a nonmalignant human mammary epithelium using CRISPR-Cas9 technology. The 2 clones exhibited undetectable *PRAME* expression, with significantly increased proliferation, invasion, and migration potential compared with the native cell line (supplementary methods; Fig. S4). We assessed the mRNA expression of several markers linked to cell cycle, apoptosis, and epithelial-to-mesenchymal transition. As for *P16/CDKN2A*, *P21/CDKN1A*, *TP53*, *BAX*, and *BCL2*, we did not see any difference between the native cell line and the *PRAME* KO clone. In contrast, *CDH1* (epithelial marker) significantly decreased, while *ZEB1* (transition

marker) and *VMN* (mesenchymal marker) significantly increased (Fig. S5, 6). After orthotopic grafting in 5 nude mice (a total of 10 nipples), and after 6 months of follow-up, we did not observe any tumor grafting.

Unlike what is observed in advanced stages, *PRAME* expression might not always be increased in the earlier stages of carcinogenesis. It could act as a driver or passenger gene depending on the carcinogenesis stage. Although we could not demonstrate the tumorigenic potential of our KO cell lines, they displayed more aggressive features than the native benign cell line, and thus the hypothesis is that completely turning-off *PRAME* gene expression initiates carcinogenesis, even in normal tissues where *PRAME* is usually expressed at very low levels.<sup>4</sup> In addition, *PRAME* being implicated in the recognition of pathogen-associated molecular patterns during an anti-microbial immune response, its loss of function could participate in evading immune destruction during early carcinogenesis. Then, *PRAME* is turned on again possibly in relation to the cancer inflammatory environment,<sup>5</sup> contributing to transforming a slowly-proliferating tumor into a more aggressive one with metastatic potential. In our patient, the constitutional *PRAME* loss might explain that none of the six cancers had metastatic evolution.

With this in-depth investigation, we highlight the success of our individual approach in the genetics of low penetrance to identify new genes of interest and potential targets. However, this approach also casts light on the limitations of demonstrating the functional value of the abnormality identified, particularly to address the question of polygenics in carcinogenesis.

## Ethics declaration

This study was approved by the local Human Research Ethics Committee. Informed consent to participate and to publish was obtained from the patient participating in the study.

## Author contributions

Conceptualization: DH, GF and GB; Data curation: DH, ME, GF and GB; Formal analysis: DH, GF, MDP and GB; Funding acquisition: AJ, GF and GB; Investigation: DH, GF, MDP and GB; Methodology: DH, GF and GB; Project administration: GF and GB; Resources: VTN, JP, CL and MEB; Supervision: GF and GB; Validation: DH, VTN, JP, CL, MEB, ME, AJ, GF, MDB and GB; Writing - original draft: DH, JP, GF and GB; Writing - review & editing: DH, VTN, JP, CL, MEB, ME, AJ, GF, MDB and GB.

## Conflict of interests

The authors declared no conflict of interests.

## Acknowledgements

We would like to thank Mrs. A. Verdier for revising the English language.

## Appendix A. Supplementary data

Supplementary data to this article can be found online at <https://doi.org/10.1016/j.gendis.2023.04.034>.

## References

1. El Bouchtaoui M, Do Cruzeiro M, Leboeuf C, et al. A constitutional activating *MET* mutation makes the genetic link between malignancies and chronic inflammatory diseases. *Clin Cancer Res.* 2019;25(14):4504–4515.
2. Epping MT, Hart AAM, Glas AM, et al. PRAME expression and clinical outcome of breast cancer. *Br J Cancer.* 2008;99(3):398–403.
3. Molnár J, Szakács G, Tusnady GE. Characterization of disease-associated mutations in human transmembrane proteins. *PLoS One.* 2016;11(3):e0151760.
4. Wadelin F, Fulton J, McEwan PA, et al. Leucine-rich repeat protein PRAME: expression, potential functions and clinical implications for leukaemia. *Mol Cancer.* 2010;9:226.
5. Wadelin FR, Fulton J, Collins HM, et al. PRAME is a Golgi-targeted protein that associates with the Elongin BC complex and is upregulated by interferon-gamma and bacterial PAMPs. *PLoS One.* 2013;8(2):e58052.

Diaddin Hamdan<sup>\*,1</sup>

Université de Paris Cité, INSERM, UMR\_S 942 MASCOT, Paris F-75006, France  
Hôpital La Porte Verte, Versailles F-78004, France

Van Tai Nguyen<sup>1</sup>

Université de Paris Cité, INSERM, UMR\_S 942 MASCOT, Paris F-75006, France  
National Cancer Hospital, Cancer Research and Clinical Trials Center, Ha Noi 100000, Viet Nam

Justine Paris  
Christophe Leboeuf  
Morad El Bouchtaoui

Université de Paris Cité, INSERM, UMR\_S 942 MASCOT, Paris F-75006, France

Marc Espié  
AP-HP-Hôpital Saint Louis, Centre de Maladies du Sein,  
Paris F-75010, France

Anne Janin  
Université de Paris Cité, INSERM, UMR\_S 942 MASCOT, Paris F-75006, France

Géraldine Falgarone  
Université de Paris Cité, INSERM, UMR\_S 942 MASCOT, Paris F-75006, France  
Université Sorbonne Paris Nord, Bobigny F-93000, France  
AP-HP-Hôpital Avicenne, Unité de Médecine Ambulatoire, Bobigny F-93000, France

Mélanie Di Benedetto<sup>2</sup>  
Université de Paris Cité, INSERM, UMR\_S 942 MASCOT, Paris F-75006, France  
Université Sorbonne Paris Nord, Bobigny F-93000, France

Guilhem Bousquet<sup>\*\*,2</sup>  
Université de Paris Cité, INSERM, UMR\_S 942 MASCOT, Paris F-75006, France  
Université Sorbonne Paris Nord, Bobigny F-93000, France  
AP-HP-Hôpital Avicenne, Service d'Oncologie Médicale, Bobigny F-93000, France

\*Corresponding author. UMR\_S942 Inserm - Université Sorbonne Paris Nord - Université de Paris, UFR SMBH, 1 rue Chablis, Bobigny F-93000, France.  
E-mail address: [diaddin.hamdan@inserm.fr](mailto:diaddin.hamdan@inserm.fr) (D. Hamdan)

\*\*Corresponding author.  
E-mail address: [guilhem.bousquet@aphp.fr](mailto:guilhem.bousquet@aphp.fr) (G. Bousquet)

10 September 2022  
Available online 30 June 2023

<sup>1</sup> Co-first authorship.

<sup>2</sup> Co-senior authorship.